Distribution of Major, Trace and Rare Earth Elements in Polymetallic Nodules of Central Indian Ocean Basin

Barman, S.K.[1], Tiwari, S.K.[2] and Kumar, G.[3]

[1]Department of Geology (Perusing PhD), Institute of Science, Banaras Hindu University, Varanasi-221005, India
[2]Department of Geology (PhD), Institute of Science, Banaras Hindu University, Varanasi-221005, India,
[3]Department of Geology (PhD), BIT Sindri, Dhanbad-828123, India

Abstract: *Polymetallic nodules from the parts (latitude 9ºS to 12ºS and longitude 76ºE to 78ºE; water depth 4,900-5,900 m) of Central Indian Ocean Basin (CIOB) reveal the presence of Mn, Cu, Ni, Zn, Co and REEs significantly. To determine the occurrence and enrichment processes of those metals high resolution mineralogical and geochemical studies were conducted.Elemental Association and correlation matrix of various elements viz. Mn, Fe, Co, Pb, Sr, Cu, Ni, Zn, and oxides viz. Na_2O, K_2O, TiO_2, CaO, P_2O_5; Al_2O_3were studied to absorb the correlation pattern and mobilization of metals in marine sediments and pore water.XRD diffraction pattern indicate presence of todorokite, vernadite (δ-MnO_2), quartz, feldspar, phillipsite and Iron. ICP-MS studies determined major and trace together with REEs distributions in nodules. Here, twenty nine elements viz. V, Cr, Mn, Co, Ni, Zn, Rb, Sr, Nb, Mo, Cs, Ba, La, Ce, Pr, Nd, Sm, Eu, Gd, Dy, Ho, Er, Tm, Yb, Lu, Hf, Pb, Th and U have been measured. Nodules display abundance of Mn (25.63%), slight Fe (8.91%) and low contents of trace elements and REEs in comparison to the common content of nodules from other oceans. Some essential elements of economic interest notably Co, Cu, Ni, Mo, Zn and REE are slightly lower in studied nodule samples than in the nodules from other oceans. The concentrations of these 29 elements within the nodules are strategic REE resource and can be used for resource exploration and could probably catalyse in adding further studies of seabed resources in the CIOB.*
Keywords: *CIOB, Geochemical Analysis, Fe-Mn (Polymetallic) Nodules, Trace Elements, REE, XRD, AAS, ICP-MS*

Introduction

The polymetallic nodules occur in the ocean basins and vary in chemical composition and abundance at the sea floor. The nodules are spread over larger area in the Pacific than in Indian and Atlantic Oceans. In this study Mn-nodule samples from the latitude 9ºS to 12ºS and longitude 76ºE to 78ºE and water depth variable from 4,900-5,900m have been considered (Fig. 1).

Bathymetric Contours (m)

-5700	-5400	-5100
-5900	-5600	-5300	-5000
-5800	-5500	-5200	-4900
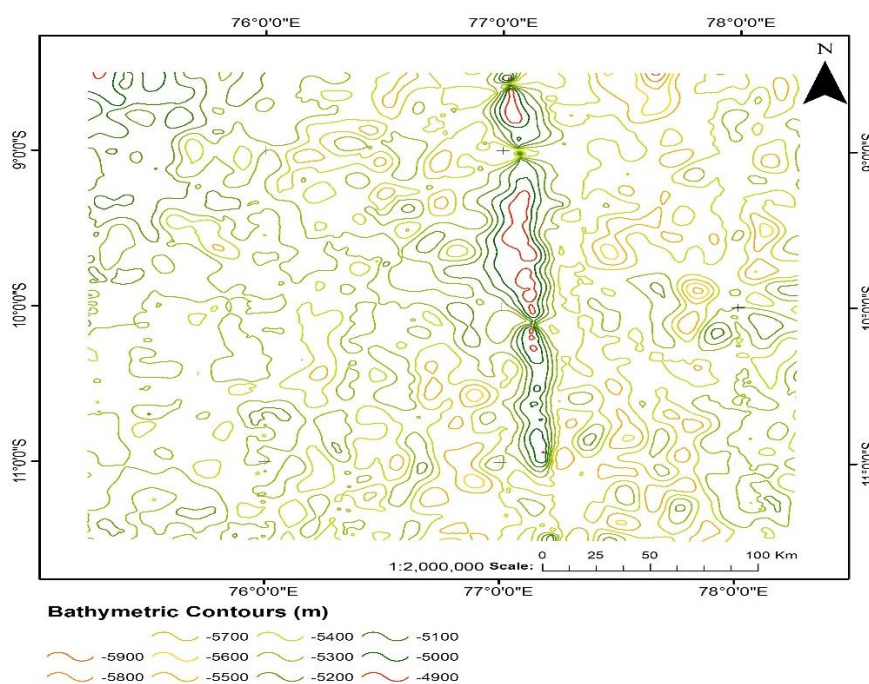
Fig. 1: Sample Location Map (Bathymetry Contour Map)

The nodules exhibit a complicated texture usually characterised through irregular, concentric micro-layers around a nucleus (Wegorzewski and Kuhn 2014). These are concretions on the sea bottom with concentric layers of iron and manganese hydroxides around a core. These are very important mineral deposits within the ocean containing many metals above crustal abundances and as a result aptly known as Fe-Mn nodules. Mn concentration is greater in nucleus of nodule and its concentration decreases in the direction of periphery. Fe-components showanoppositetrend and is more concentrated in the direction of peripheral part of nodule.

The CIOB nodules (Mn-nodules) are composed of Mn oxides and Fe oxides/hydroxides, which precipitate from the seawater or surface-sediment pore water. These nodules are rich in Mn wherein Mn/Fe ratio is excessive, however the nodules occurring in various areas have special predominant components. They incorporate a wide range of metals with high potential economic values, viz. Mn, Ni, Cu, Fe, Mo, Li, Co and REEs (Glasby et al., 1978; Halbach et al., 1981;Cronan et al., 1991;Hein et al., 2013;Hein et al. 2015;Hein and Koschinsky 2014a;Bau et al. 2014b). Although, preceding research have targeted at the morphology, mineralogical and geochemical compositions (Halbach et al. 1982;Nath et al. 1992;Pattan and Banaker 1993;Hlawatsch et al., 2002;Verlaan et al., 2004;Cronan 2006;Takahashi et al. 2007), yet a detailed study of the nodules of CIOB are needed, which may reflect the growth processes leading to various genetic types of nodules: hydrogenetic and diagenetic precipitation (Reyss et al. 1985;Wegorzewski and Kuhn 2014). The REE content within the nodules are more than marine sediments and seawater. Usually, the REE content is 10 to 100 times greater than in deep-sea sediments or seawater (Zhang et al. 2012a).

The researches associated with the nodules of Pacific Ocean is extensive and numerous works have been published discussing numerous primary issues by Horn et al. 1972;GP Glasby 1977;Burns and Burns 1977a. On the other hand, there have been limited works at the Indian Ocean nodules(Bezrukov and Andrushchenko 1974;Cronan 1977;Siddiquie et al. 1978;Frazer and Wilson 1980;Cronan and Moorby 1981) until 1982 when serious scientific expeditions started regularly and systematically in CIOB. Since then several research papers have been published discussing biology (Parulekar et al., 1982), reserves (Siddiquie et al., 1984), morphology (Mukhopadhyay 1987), mineralogy (Rao 1987), topography (Pattan and Kodagali 1988), and geochemistry and formation of various sized CIOB nodules (Valsangkar and Khadge 1989).

I.   Materials and Methods

Sample, Reagents: Samples of Mn-nodules, have been acquired from CIOB. Sampling was carried out by boomerang grabs throughout cruise attachment GA-REAY-1-1985. Different size nodules were taken for the study looking on availability. The samples were selected on the basis of their color, external morphology and size. The chosen samples were reduced vertically in two halves with relevance to their position on the seafloor earlier than macroscopically internal descriptions and physical, XRD and chemical analysis.

Owing to the availability of modern fine-scale analytical instruments viz. XRD, AAS, HR-SEM, and ICP-MS, geochemical and mineral compositions have been studied. The mineral compositions have been determined by X-ray Powder Diffraction (XRD) using fine powder of Fe-Mn nodule to gather diffraction patterns. HR-SEM ((Model: Nova Nano SEM 450, FEI of USA (S.E.A.) PTE, LTDEDS: Pegasus Integrated EDS-EBSD with Octane Plus and Hikari Pro: EDAX Inc.) was used to a wide range of floor analysis.

The methodology includes the experimental layout and methods adopted throughout the study. Twenty nine dried nodules samples were taken into consideration. The samples were crushed for bulk analyses. These samples were reduced into two halves and were polished and used for mineralogical research. The dry samples were carefully crushed and ground in an agate mortar (non-abrasive disaggregation process). The samples were then sieved using sieves of 63μ. The sieved samples so obtained were washed completely by distilled water. Then those were dried in an oven at 110º C for three hours. The powdered samples were used for mineralogical studies by XRD. Some components of the samples was used for chemical evaluation and for leaching analysis.

Major and trace (together with REE) elements concentrations were analyzed by Atomic Absorption Spectrophotometer (AAS) (Table 1). In chemical analysis 0.5g of samples was used with NaOH pellets in Ni crucible and the material was transferred into 250 ml flask. With the assistance of 1:1 HCl the quantity was made 250 ml. This acts as solution A and was used for SiO_2 and Al_2O_3 analysis through U-V spectrophotometer.

Then, 0.1g of sample was taken for the preparation of solution B through acid digestion. This sample was kept in the tephelon bomb observed through including few drops of HF, HCl and HNO_3. The sample was digested for approximately 2 hours and transferred into 100 ml flask with the assistance of 1:1 HCl and made the quantity 100 ml. This solution was used for numerous trace and major elements analysis through AAS using

Perkin Almer model 2380. A part of this solution was conjointly used for the determination of TiO_2 and P_2O_5 through U-V spectrophotometer. Elemental composition of Mn, Fe, Cu, Ni, Co and Zn was determined using AAS of the samples.

S. No	Morphology & Surface Texture	Mn%	Fe%	SiO2%	Al2O3%	CaO%	MgO%	Na2O%	K2%	Cu%	Ni%	TiO2 ppm	P2O5 ppm	Zn ppm	Co ppm	Pb ppm	Sr ppm
1.	m(S-E)s	25.25	8.12	13.41	2.94	2.11	1.74	1.28	0.89	1.12	1.01	7400	2500	1800	2000	1000	600
2.	s(S-E)r	27.14	7.98	14.12	3.11	2.36	1.82	1.33	0.91	1.18	1.12	7600	2800	1600	1900	1200	700
3.	m(P)s	25.23	3.11	14.21	3.12	2.42	1.88	1.35	0.92	1.04	0.99	7900	2900	1600	2000	1400	900
4.	m(D)r	26.29	8.04	13.82	2.98	2.14	1.72	1.45	0.98	1.16	1.18	7600	2300	1700	1900	900	900
5.	s(S)r	28.42	7.76	13.96	3.14	2.16	1.88	1.35	0.94	1.21	1.19	7200	2400	1900	1700	800	1000
6.	s(S)s	27.41	7.98	14.72	3.22	2.12	1.99	1.48	1.02	1.19	1.14	7300	2200	1700	1800	1000	600
7.	m(B)s	24.98	9.88	16.12	3.55	2.58	1.98	1.56	1.12	1.06	0.98	7700	3500	1400	2500	1500	1300
8.	m(D)s	24.51	9.91	16.51	3.31	2.62	1.95	1.63	1.18	1.03	0.99	7800	3200	1400	2500	1700	1400
9.	m(B)s	24.48	10.11	15.15	3.12	2.38	1.64	1.45	1.12	1.04	0.99	8300	2800	1500	2800	1800	900
10.	m(D)r	25.76	9.38	15.24	3.15	2.46	1.97	1.73	1.17	1.08	1.01	8100	3400	1500	2300	1500	800
11.	s(E)r	27.98	8.92	14.92	2.92	2.21	1.84	1.75	1.19	1.10	1.08	8000	2600	1600	2200	1200	800
12.	s(B)r	26.72	9.17	15.86	3.54	2.61	1.94	1.72	0.92	1.12	1.07	8300	3800	1500	2100	1000	1100
13.	s(E)r	28.42	7.97	14.14	2.95	2.18	1.74	1.32	0.98	1.22	1.15	8200	2700	1900	1800	900	600
14.	s(S)r	27.46	7.98	15.14	3.12	2.51	1.92	1.41	1.09	1.19	1.14	7400	3400	1800	1800	900	1100
15.	m(B)s	24.42	9.41	12.78	2.92	2.32	1.81	1.31	1.03	1.02	0.98	7800	2200	1400	2500	1700	1000
16.	m(D)s	27.42	8.14	13.92	3.09	2.41	1.72	1.22	1.02	1.19	1.18	7600	2800	1800	2000	1200	1200
17.	s(S)r	26.12	8.66	14.16	3.21	2.46	1.98	1.25	0.99	1.18	1.16	7500	3200	1600	2200	1600	1300
18.	s(S)r	28.92	7.92	15.11	3.52	2.52	1.76	1.32	1.11	1.22	1.24	6800	3600	1700	1600	1100	700
19.	l(E)s	23.62	9.64	14.72	3.02	2.51	1.71	1.41	1.07	1.01	0.98	7800	3400	1500	2600	1400	1300
20.	l(E)s	24.12	9.72	13.73	2.98	2.47	1.48	1.56	1.11	1.04	0.97	8100	3300	1400	2500	1600	1200
21.	l(D)r	25.72	9.11	14.71	3.16	2.31	1.44	1.62	1.13	1.08	1.02	8000	2800	1700	2200	1400	1200
22.	l(S)r	25.45	9.09	14.35	3.18	2.49	1.58	1.78	1.21	1.08	1.04	7800	3200	1600	2100	1100	1400
23.	l(B)s	22.94	10.11	15.68	3.63	2.75	1.95	1.71	1.11	1.01	0.98	8000	3600	1500	2800	1800	1600
24.	l(B)s	23.38	9.79	15.54	3.58	2.54	1.91	1.68	1.09	1.04	0.98	7500	3100	1400	2400	1500	1400
25.	l(B)r	24.65	9.14	14.98	3.21	2.23	1.78	1.66	1.05	1.08	1.04	7400	2400	1600	2200	1400	900
26.	l(S)s	23.62	10.01	15.91	3.64	2.82	1.99	1.69	1.07	1.02	0.98	7900	3500	1500	2500	1800	1500
27.	l(E)r	24.24	9.99	15.01	3.11	2.76	2.04	1.74	1.18	1.05	1.02	8000	3400	1500	2400	1700	1600
28.	l(P)s	23.78	10.12	15.98	3.68	2.41	1.58	1.77	1.19	1.04	0.99	8300	2700	1600	2500	1500	1300
29.	l(D)r	25.61	9.74	14.65	3.11	2.65	1.88	1.65	1.04	1.11	1.08	7800	3600	1600	2400	1400	1500
30.	l(B)s	24.91	10.5	15.76	3.65	2.46	1.67	1.76	1.11	1.05	0.97	8400	2800	1400	2600	1700	1300
SD		1.66	1.39	0.87	0.25	0.19	0.16	0.19	0.09	0.07	0.08	372.4	468.7	149.4	326.9	310.4	308.0
Average		25.63	8.91	14.81	3.23	2.43	1.81	1.53	1.06	1.10	1.05	7783	3003	1590	2227	1357	1103

Table-1 Chemical Analysis of the Manganese Nodules using AAS from Parts of Central Indian Ocean Basin

In the present study the digested samples, and blanks were analysed using the *Agilent Quadrapole 7700 ICP-MS* facility installed at the Birbal Sahni Institute of Paleaoscinces (BSIP), Lucknow, India for trace element concentrations. All the dataset shows results within the limit of 5% error. The reproducibility of repeated samples was within the error. Approximately 30 mg powdered of every representative sample was taken to carry out Trace and Rare Earth Element analyses. The digestion of the sample was done in a Teflon tube using a two-step digestion system. In the primary step, combination of hydro fluoric acid and nitric acid ($HF+HNO_3$ in 2:1 ratio) along with 1 ml perchloric acid ($HClO_4$) was added in the sample, then the tube was tightly capped and heated to ~120°C for 7 hours (Q-Block operating system). Afterwards, the lid of the Teflon tube was loosened to permit evaporation of acid fumes and persevered till the acid fumes stopped evaporating from the tube, and the sample dried completely. In the following step, the same process was repeated with opposite ratio combination of hydrofluoric acid and nitric acid ($HF+HNO_3$ in 1:2 ratio) along with 1 ml perchloric acid ($HClO_4$). Subsequently, the tube was checked for entire digestion of nodules sample by adding 2 ml of 5% HNO_3 and observing the clarity of the solution. If any part was still left, the process was repeated till its entire digestion. After that, 2% HNO_3 solution was used to rinse every tube, and the sample was transferred in a volumetric flask to make the final volume of 50ml. Thus, during this study, we acquired high resolution chemical data of polymetallic nodules. The mineralogy of the various size category of nodules followed by their analysis for major, trace including RREs to recognize the occurrence and enrichment processes of the economic metals of the nodules have been carried out.

II. Results and Discussion

3.1 HR-SEM analysis: The nodules samples were analyzed using High Resolution Scanning electron microscopy (HR-SEM) at (CIF) IIT-BHU, Varanasi; HR-SEMEDS: Nova Nano SEM 450: FEI Company of USA (S.E.A) PTE, LTDEDS: Team Pegasus Integrated EDS-EBSD with Octane Plus and Hikari Pro: EDAX Inc. with a centred electron beam produced by a field emission gun using a 15 kV acceleration. The HR-SEM incorporates a beam size of 1 to 100 μm and 500 nm diameter with a maximum 20 KX magnification and resolution (eV) 125.3.

The primary components of nodules are: goethite, lepidocrocite, 7A°& 10A° manganates, pyrolusite, quartz and phyllosilicates. Accessory minerals accompanying these major phases include calcite, dolomite, siderite, rhodochrosite, pyrite, marcasite, chalcopyrite, potassium feldspar, zircon, rutile, ilmenite, apatite and chlorite. Gypsum is present as a trace secondary mineral. Fe-Mn oxides and oxyhydroxides represent a mean of >70 wt% of the nodular mass and they form an important part of the layers. Nuclei are composed of carbonates (essentially siderite to rhodochrosite), silicates in minor proportion and disseminated pyrite as an accessory mineral. Silicates (especially in detrital layers) and carbonates distributed within the oxide layers and concentrated within the nuclei represent approximately 30 wt% of the nodular mass.

The HR-SEM spectrum of small nodule indicates high values of V, Ti, Mn and Fe and low value of Mo, Th, Ti, V, Co, Ni, Cu and Zn (Fig. 2a). The O, Cr, Mn and Ti content display high values in the medium nodules whereas the low value of Ni, Co, Ti, Zn, Cu and Fe (Fig. 2b). Similarly the value of Fe, Cu, Co and Cr is high in large nodules while there are low values of Ti, Ni and Mn (Fig. 2c). In general, the value of Mn is higher in an exceedingly small and medium nodule compared to larger ones.

Lsec: 30.0 0 Cnts 0.000 keV Det: Octane Plus Det
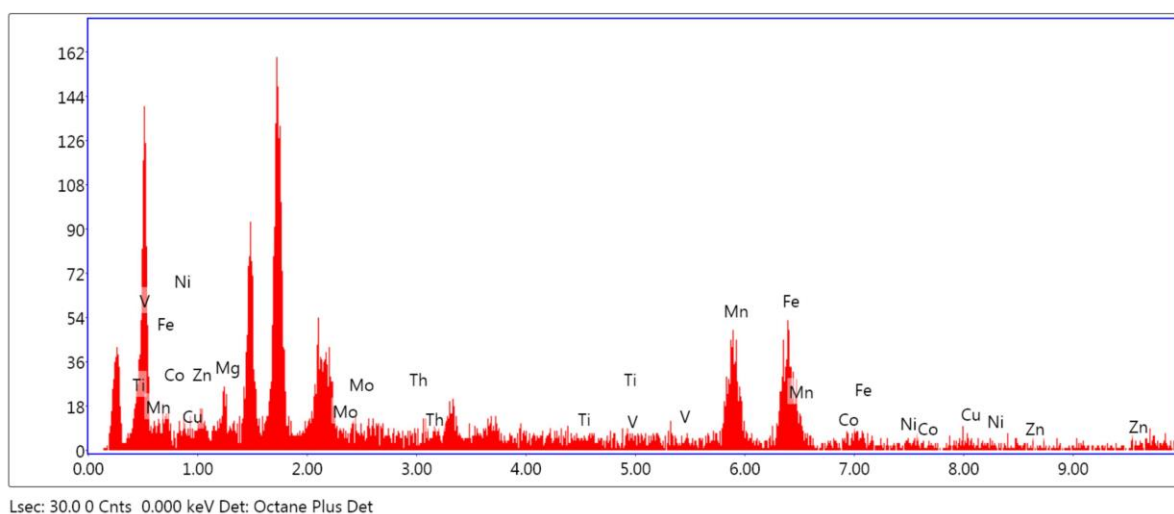
Fig. 2 a: *HR-SEM Plot of Small Nodules (0-3 cm)*
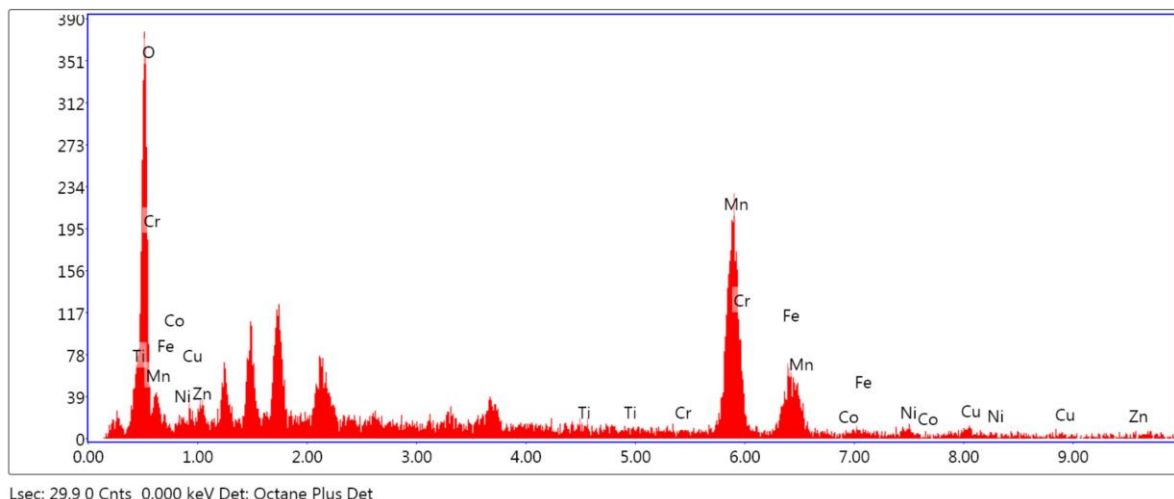
Fig. 2 b: *HR-SEM Plot of Medium Nodules (3-6 cm)*
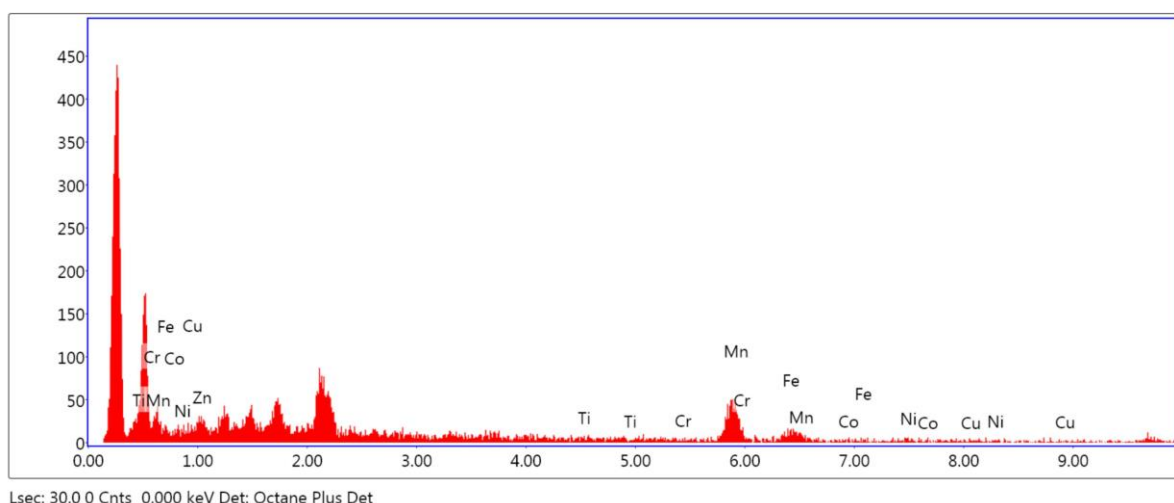
Fig. 2 c: *HR-SEM Plot of Large Nodules (>6 cm)*

3.2 XRD analysis: The mineral compositions of Fe-Mn nodules especially manganese oxide and other accessory mineral phases were determined by X-ray Powder Diffraction (XRD) pattern using fine powder of Fe-Mn nodule to gather diffraction patterns. Mineralogical X-ray diffraction (XRD) profiles from $2\theta=3\text{-}60°$ (40kV and 15 mA) in 0.0200 steps have been acquired for 08 samples using Model: Rigaku Smart Lab 9kW Powder type (without χ cradle), RIGAKU Corporation at (CIF) IIT-BHU, Varanasi, India. The Fe-Mn nodules incorporate high concentration of Mn. The major minerals within the nodules, recognized through XRD pattern, are vernadite, toderokite, birnessite, phillipsite, goethite, akaganeite, and the minor minerals in the nodules encompass montmorillonite, barite, gypsum, *a*-cristobalite, kaolinite, quartz, feldspar, and others.

XRD analysis yielded comparable X-ray powder diffraction patterns for the polymetallic nodules (small, medium, large) analyzed. The diffraction peaks of nodules particularly correspond to todorokite, vernadite (δ-MnO_2), quartz, Phillipsite and Feldspar (Fig. 3a, b, c). Infact crystallinity is not very good therefore the peaks are not very high, clear and well defined. The nodules include moderate concentrations of Fe and no reflections of Fe-phase minerals were recorded within the nodules. This can be because of bad crystallinity (X-ray amorphous) of Fe oxides/hydroxides. It is tough to estimate the percentage of each phase due to the presence of amorphous phase. However, the major Mn mineral is vernadite, which is common in most marine hydrogenetic manganese oxides (Hein et al. 2013;Hein et al. 2016), and minor quantities of todorokite in nodules. The todorokite has a relatively high crystallinity and suggests obvious sharp X-ray reflection, contrasting vernadite, which suggests an extensive and weak X-ray reflection, suggesting that vernadite has bad crystallinity. The high peak corresponds to quartz although lesser in quantities and also other detrital minerals viz. feldspar, Phillipsite etc. shows that possible terrigenous detrital supply is far away. However, todorokite in affiliation with quartz,

feldspar and phillipsite is observed within the nodules. The Preliminary result shows that Mn released from smectite clay mineral and early diagenesis are responsible for their formation.
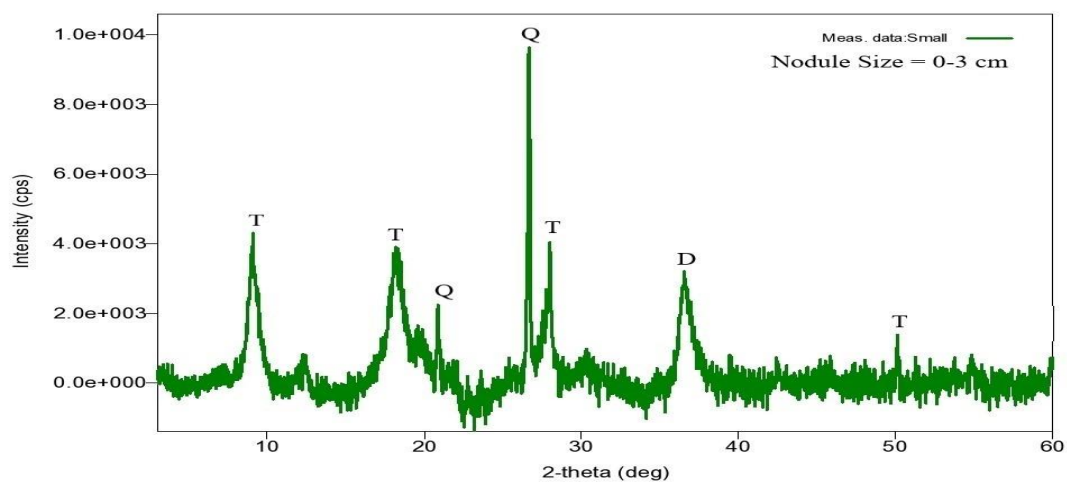
Fig. 3 a: *XRD pattern of small size nodules (0-3 cm)*
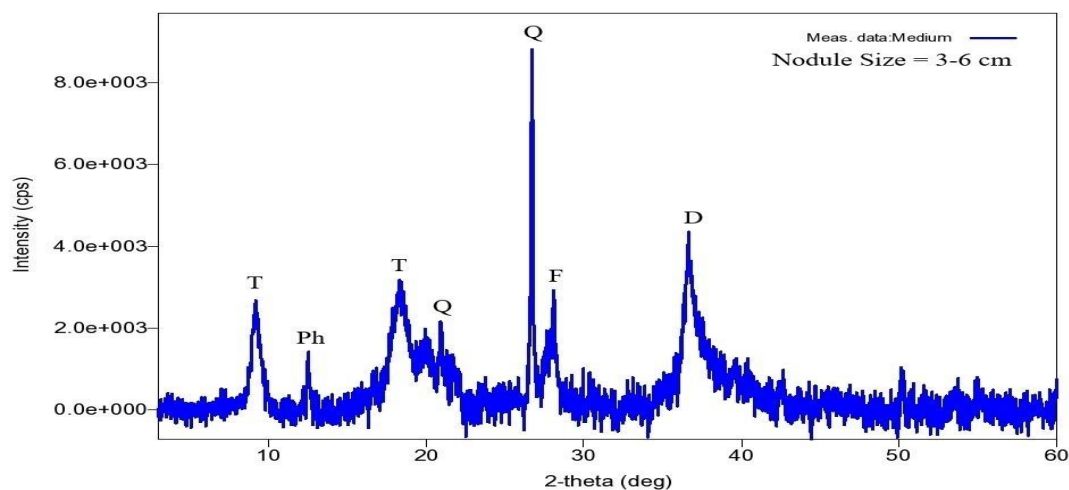
Fig. 3 b: *XRD pattern of medium size nodules (3-6 cm)*
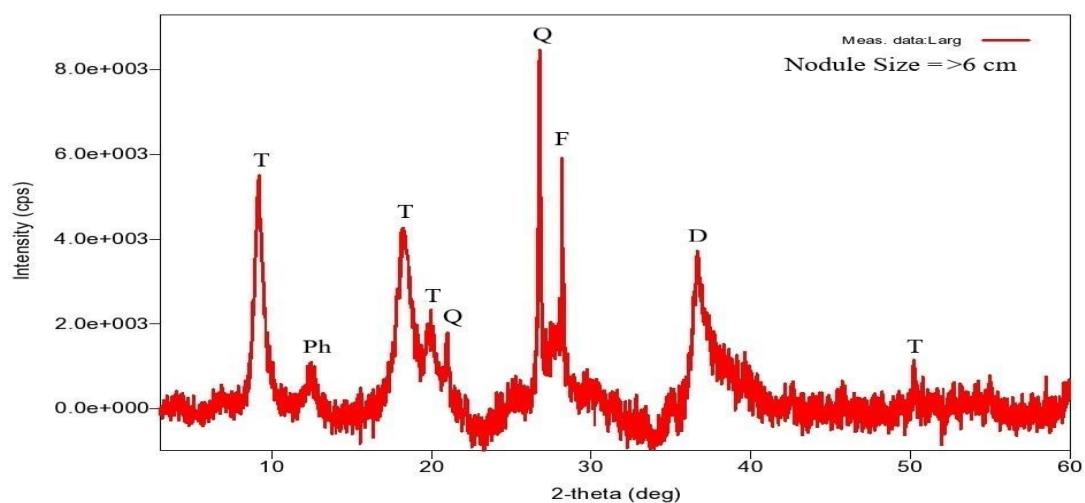
Fig. 3 C: *XRD pattern of large size nodules (>6 cm)*

Todorokite and delta MnO_2 are the two essential minerals present within the nodules. Generally, nodules rich in manganese have todorokite and those rich in iron have δ-MnO_2. The X-ray diffraction pattern of

08 nodule samples suggests small and huge peaks of todorokite in small size nodules. The major Mn minerals viz. todorokite, δ-MnO$_2$ (vernadite) and Quartz occur as an important minerals (Fig. 3a). In smaller nodules occurrence of phillipsite and feldspars is less and that of birnessite is rare. The important mineral within the medium size nodules are todorokite, δ-MnO$_2$ (vernadite), Feldspar, phillipsite and Quartz (Fig. 3b). It has been observed that the profile peaks of todorokite decreases from small to larger size nodules with few exceptions as seen in the XRD profile of large nodules (Fig. 3c). These mineral phases are intergrown with the X-ray amorphous Fe oxides/hydroxides, which may have been crystallized to goethite (Hein and Koschinsky 2014a). Additionally, detrital aluminosilicate minerals such as quartz and minor feldspars are present in the nodules.

The relationship between Mn and Ni content in Fe-Mn nodules illustrate the mineralogical control on minor metal concentration. Infact, the higher Mn and Ni content illustrate the concentration of todorokite as the principle Mn mineral and lower percent of Mn, Fe represent the δ-MnO$_2$. Besides this todorokite is also found at greater depth whereas δ-MnO$_2$ is found at lesser depth.

Hydrogenetic polymetallic nodules are primarily composed of vernadite (δ-MnO$_2$), thatis intergrown with X-ray amorphous Fe-oxyhydroxide (Hein et al.,2000;Koschinsky et al. 2010). During the diagenetic growth, the nodules develop different manganese minerals, 7Å and 10Å manganates viz. todorokite, phyllomanganates (Burns et al. 1978b;Burns et al. 1978a), buserite (Usui & Someya 1997), and birnessite (Usui, A & Someya 1997;Hein et al. 2013a). X-ray amorphous Fe oxyhydroxides have been also reported to contain feroxyhyte, ferrihydrite and goethite (Baturin 1988).

Mn show a strong negative correlation with Fe, Co, Pb, Sr; Fe show a strong negative correlation with Cu, Ni, Zn; Cu show strong negative correlation with Co, Pb, Sr, CaO, Na$_2$O, TiO$_2$; Ni show a strong negative correlation with Co, Pb, Na$_2$O, TiO$_2$ while Zn show a strong negative correlation with Co, Pb, Sr, CaO, Na$_2$O. Similarly, Mn show a strong positive correlation with Cu, Ni, Zn; Fe show a strong positive correlation with Co, Pb, Sr, CaO, Na$_2$O, K$_2$O, TiO$_2$; Cu show a strong positive correlation with Ni, Zn; Ni show a strong positive correlation with Zn; Co show a strong positive correlation with Pb, Sr, CaO, TiO$_2$; Pb show a strong positive correlation with Sr, CaO; Sr show a strong positive correlation with CaO, Na$_2$O, P$_2$O$_5$; Al$_2$O$_3$ show a strong positive correlation with CaO; CaO show a strong positive correlation with P$_2$O$_5$; Na$_2$O show a strong positive correlation with K$_2$O, TiO$_2$. (Table: 2).

Table 2: Correlation Matrix of the Manganese Nodules from Parts of CIOB (All Size Class)															
	Mn	Fe	Cu	Ni	Zn	Co	Pb	Sr	SiO2	Al2O3	CaO	MgO	Na2O	K2O	TiO2	P2O5
Mn	1															
Fe	-0.817	1														
Cu	0.94	-0.847	1													
Ni	0.873	-0.803	0.944	1												
Zn	0.722	-0.815	0.791	0.746	1											
Co	-0.857	0.942	-0.868	-0.829	-0.792	1										
Pb	-0.783	0.837	-0.797	-0.724	-0.791	0.878	1									
Sr	-0.631	0.705	-0.581	-0.441	-0.502	0.629	0.582	1								
SiO2	-0.0829	0.24	-0.136	-0.196	-0.241	0.217	0.21	0.122	1							
Al2O3	-0.318	0.456	-0.298	-0.242	-0.379	0.302	0.343	0.451	0.325	1						
CaO	-0.491	0.629	-0.505	-0.383	-0.573	0.523	0.591	0.786	0.0288	0.551	1					
MgO	0.0251	0.013	0.0052	0.0138	-0.142	-0.0425	0.0246	0.0689	-0.155	0.208	0.345	1				
Na2O	-0.449	0.695	-0.517	-0.525	-0.518	0.499	0.37	0.503	0.235	0.478	0.435	0.118	1			
K2O	-0.333	0.62	-0.419	-0.373	-0.431	0.49	0.469	0.456	0.0941	0.256	0.393	-0.106	0.655	1		
TiO2	-0.418	0.613	-0.528	-0.598	-0.431	0.621	0.459	0.289	0.313	0.106	0.248	-0.195	0.515	0.297	1	
P2O5	-0.214	0.397	-0.24	-0.176	-0.369	0.281	0.283	0.549	-0.0803	0.429	0.866	0.248	0.321	0.287	0.15	1

Mn shows strong positive correlation with Cu and Ni in medium and large nodules while it also shows strong negative correlation with Fe in small nodules. Fe shows strong negative correlation with Cu and Ni in small and large nodules. Cu shows strong positive correlation with Ni in all size nodules (Table: 3, 4 & 5).

In %	Mn	Fe	SiO_2	Al_2O_3	CaO	MgO	Na_2O	K_2O	Cu	Ni
Mn	1									
Fe	-0.54662	1								
SiO_2	-0.10004	0.53981	1							
Al_2O_3	-0.1294	0.184287	0.596182	1						
CaO	-0.37623	0.385081	0.614206	0.682819	1					
MgO	-0.74466	0.332906	0.193492	0.210202	0.119187	1				
Na_2O	-0.10006	0.715754	0.684682	0.052079	0.039101	0.199159	1			
K_2O	0.377441	0.105667	0.309029	-0.20665	-0.041	-0.16947	0.300491	1		
Cu	0.426287	-0.8826	-0.51567	0.031642	-0.17367	-0.30414	-0.87984	-0.22737	1	
Ni	0.530208	-0.70709	-0.35596	0.239747	-0.02512	-0.31144	-0.75951	0.077816	0.846115	1

Table No: 3 Correlation Matrix for Small Size Nodules (0-3 cm)

In %	Mn	Fe	SiO_2	Al_2O_3	CaO	MgO	Na_2O	K_2O	Cu	Ni
Mn	1									
Fe	-0.23705	1								
SiO_2	-0.26781	0.354908	1							
Al_2O_3	-0.19039	0.248567	0.877773	1						
CaO	-0.23965	0.205366	0.801257	0.826642	1					
MgO	-0.24227	0.012579	0.572109	0.655629	0.68966	1				
Na_2O	-0.2903	0.407391	0.7808	0.576751	0.553093	0.667748	1			
K_2O	-0.26744	0.698664	0.772449	0.608611	0.74823	0.456045	0.790102	1		
Cu	0.918867	-0.08717	-0.33846	-0.29005	-0.48159	-0.43149	-0.36864	-0.3784	1	
Ni	0.884975	-0.10454	-0.32856	-0.31887	-0.39829	-0.46929	-0.33464	-0.27522	0.906469	1

Table No: 4 Correlation Matrix for Medium Size Nodules (3-6 cm)

In %	Mn	Fe	SiO_2	Al_2O_3	CaO	MgO	Na_2O	K_2O	Cu	Ni
Mn	1									
Fe	-0.4981	1								
SiO_2	-0.46791	0.62568	1							
Al_2O_3	-0.45447	0.616773	0.917833	1						
CaO	-0.42246	0.523558	0.27441	0.221941	1					
MgO	-0.45049	0.389991	0.461285	0.284566	0.750002	1				
Na_2O	0.13546	0.271251	0.476093	0.580399	0.151141	0.189548	1			
K_2O	0.09964	-0.00651	-0.01272	0.069759	-0.03105	-0.31048	0.540408	1		
Cu	0.89307	-0.51979	-0.40311	-0.39534	-0.39537	-0.23543	0.237644	-0.0123	1	
Ni	0.709259	-0.55335	-0.35512	-0.45997	-0.12576	0.067526	0.154056	-0.05434	0.872659	1

Table No: 5 Correlation Matrix for Large Size Nodules (>6 cm)

3.3 ICP-MS Analysis: In oceanic mineral studies and development, geochemical analysis is one of the key technology. The deep sea nodules are among the most important potential deep-sea mineral resource. These nodules are shaped in a unique environment and are rich in Cu, Co, Ni, REE (rare earth elements in addition to water and salts (Yao et al., 1993;Yao et al., 1996;Wiltshire et al. 1999;Xia et al., 2001). Earlier, while the composition of Fe-Mn nodules was used to be analysed through traditional methods, interelemental interferences were common and very serious.

Presently, ICP-MS is rapidly becoming one of the most effective elemental analytical technology since it was invented two decades ago, having high sensitivity, low detection limits and contemporary and simultaneous analysis of multielements. In the ''standards'' series of the US Environmental Protection Administration (EPA), ICP-MS has been indexed as a preferred method of analysis for inorganic metals in samples. At present, more than 60 elements present in maximum rocks, minerals, soils, sediments, and waters are determined using ICP-MS, and its reliability is accepted worldwide. In 1997, Jarvis et al. systematically introduced the history, principle, and applications of ICP-MS technology which are successfully applied in multielemental determination in geological and environmental samples. With the development and current advances in analytical technology, the International Seabed Authority (ISA) has also recommended that the concentrations of micro and trace elements in these nodule be determined using ICP-MS.

The nodules are marine authigenic sedimentary rocks that occur at the bottom of ocean basins. Minerals in those nodules are very fine, the size of most authigenic Fe-Mn oxyhydroxide minerals are less than 300A° (Shan and Yao 1993). The mineralogical characteristics determine that dissolution of Fe-Mn nodules is relatively easy, and ICP-MS technology can overcome the interelemental interference. Therefore, this technology has a unique predominance over other techniques in the determination of elements in Fe-Mn nodules. During this study, we have used this effective analytical method for V, Cr, Mn, Co, Ni, Zn, Rb, Sr, Nb, Mo, Cs, Ba, La, Ce, Pr, Nd, Sm, Eu, Gd, Dy, Ho, Er, Tm, Yb, Lu, Hf, Pb, Th and U present in these nodules by ICP-MS (Table 6). The Table 7 indicates positive & negative correlation matrix between elements. The conditions and sample experiments using ICP-MS indicates that this procedure is a good experimental method with the characteristics of correct principle, clear interference, smooth operation, reliable and authentic results.

Table 6: Trace & REE data analysed by ICP-MS (Values in ppm)			
Elements	**Small (ppm)**	**Medium (ppm)**	**Large (ppm)**
51 V	330.5897	329.3378	312.4833
52 Cr	10.0504	50.37876	17.22575
55 Mn	214661.1	185995.4	194807.7
59 Co	1224.243	1247.172	1162.814
60 Ni	9753.826	6389.456	8521.592
66 Zn	1064.298	808.1615	925.1541
85 Rb	13.96983	13.67957	14.40114
88 Sr	566.0252	623.7994	563.5099
93 Nb	10.59904	11.68329	12.67091
95 Mo	295.0816	264.6688	286.8595
133 Cs	0.593327	0.597298	0.639837
137 Ba	1108.119	1197.054	1401.958
139 La	98.09463	137.6102	99.32144
140 Ce	462.168	647.4192	497.1779
141 Pr	27.2587	34.93257	27.34803
146 Nd	109.6557	142.0971	110.9054
147 Sm	28.60107	32.63617	25.74193
153 Eu	6.497669	8.221376	6.52056
157 Gd	27.33126	35.71322	26.68173
163 Dy	21.25498	29.07438	21.07813
165 Ho	3.973193	5.653612	3.902705
166 Er	10.48849	15.53923	10.60373
169 Tm	1.556964	2.264289	1.61723
172 Yb	9.881653	15.01184	10.079
175 Lu	1.490469	2.320323	1.549698
178 Hf	2.222095	2.267515	3.077054
208 Pb	615.3371	734.1352	670.6896
232 Th	26.175	27.92025	27.05569
238 U	3.724045	4.135673	3.640038
Total Value	230494.21	198808.35	209574.00
Mean	7948.076	6855.46	7226.69
SD	39797.49	34474.32	36111.69

III.   REEs in polymetallic nodules

REEs are strategic materials needed for growth of advance cutting-edge defence technology. They might change traditional industries, and hence, are believed to be a significant important resource in 21st century. On land, rare earth elemental resources are decreasing. However, rich deposits of REEs are often found in marine nodules. The present measurement of REEs examine single element. Since the growth of submarine technology, research into Fe-Mn nodules has become more sophisticated and advance. Now, enhanced methods of separating the linked Fe, Mn, Cu, Co, and Ni from those nodules would definitely increase the human ability to develop and use REEs. Developments in rare earth mineral dressing and smelting technology have and can still to cause quality requirements to decrease, however this only renders ocean polymetallic nodules with REEs more attractive.

Amount of REE is very low within the ocean water. The content in the surface water being the lowest, and total amount of REE increases with depth (Dubinin and Shirshov 2004;Elderfield et al., 1988;Baar et al. 1985;Alibo and Acta 1999). Marine sediments gather REEs over time, absorbing them from seawater, and the REE content in the oceanic sediments can reach 468.26×10^{-6} (Xu et al., 2007;Sholkovitz 1988;Sholkovitz 1990;Sholkovitz et al. 1994). This value is higher than those recorded in Earth's dry-land crust and sedimentary rocks. This REE enrichment is particular controlled by the absorption of Fe-Mn oxides and clay minerals in the nodules and the high levels of REEs in seawater and sediments. High cerium enrichment in nodules may lead to more effective exploitation of REEs in future (Zhang et al. 2012b).

Some critical elements of economic interest notably Co, Cu, Ni, Mo, and Zn decrease within the nodules of CIOB than in the nodules from Pacific mineralization zones. Concentrations of Mn, Pt, Mo, Co, Te, and Bi, however, show comparatively high concentrations relative to the continental crust (Guan et al. 2017a)**.**

Table 7: Correlation Matrix of elements analyzed by ICP-MS of Manganese Nodules from Parts of Central Indian Ocean Basin (Minor, Trace & REE)

	V	Cr	Mn	Co	Ni	Zn	Rb	Sr	Nb	Mo	Cs	Ba	La	Ce	Pr	Nd	Sm	Eu	Gd	Dy	Ho	Er	Tm	Yb	Lu	Hf	Pb	Th	U
V	1																												
Cr	0.29	1																											
Mn	0.277	-0.839	1																										
Co	0.947	0.583	-0.0471	1																									
Ni	-0.0911	-0.979	0.932	-0.407	1																								
Zn	0.112	-0.919	0.986	-0.214	0.979	1																							
Rb	-0.89	-0.694	0.191	-0.989	0.535	0.354	1																						
Sr	0.478	0.979	-0.711	0.736	-0.918	-0.819	-0.826	1																					
Nb	-0.883	0.193	-0.696	-0.685	-0.387	-0.565	0.572	-0.00997	1																				
Mo	-0.196	-0.995	0.888	-0.501	0.994	0.953	0.621	-0.955	-0.287	1																			
Cs	-1	-0.275	-0.292	-0.942	0.0761	-0.127	0.883	-0.465	0.89	0.181	1																		
Ba	-0.972	-0.0565	-0.495	-0.844	-0.146	-0.342	0.758	-0.258	0.969	-0.0403	0.975	1																	
La	0.421	0.99	-0.755	0.691	-0.942	-0.855	-0.788	0.998	0.0542	-0.972	-0.407	-0.195	1																
Ce	0.279	1	-0.845	0.573	-0.982	-0.923	-0.686	0.977	0.204	-0.996	-0.265	-0.0452	0.989	1															
Pr	0.436	0.988	-0.744	0.703	-0.936	-0.845	-0.798	0.999	0.0371	-0.968	-0.423	-0.212	1	0.986	1														
Nd	0.415	0.991	-0.759	0.686	-0.944	-0.858	-0.784	0.997	0.0609	-0.974	-0.401	-0.189	1	0.99	1	1													
Sm	0.775	0.829	-0.392	0.937	-0.7	-0.541	-0.978	0.925	-0.388	-0.771	-0.766	-0.605	0.899	0.823	0.907	0.896	1												
Eu	0.435	0.988	-0.745	0.702	-0.936	-0.846	-0.798	0.999	0.0385	-0.968	-0.421	-0.211	1	0.986	1	1	0.906	1											
Gd	0.502	0.973	-0.692	0.754	-0.907	-0.803	-0.841	1	-0.0376	-0.946	-0.489	-0.285	0.996	0.971	0.997	0.995	0.936	0.997	1										
Dy	0.463	0.983	-0.724	0.724	-0.925	-0.829	-0.816	1	0.00755	-0.96	-0.449	-0.241	0.999	0.98	1	0.999	0.919	1	0.999	1									
Ho	0.477	0.979	-0.712	0.735	-0.919	-0.82	-0.825	1	-0.00865	-0.955	-0.464	-0.257	0.998	0.977	0.999	0.998	0.925	0.999	1	1	1								
Er	0.427	0.989	-0.75	0.696	-0.939	-0.851	-0.792	0.998	0.0469	-0.97	-0.414	-0.203	1	0.987	1	1	0.902	1	0.996	0.999	0.998	1							
Tm	0.375	0.996	-0.787	0.654	-0.957	-0.879	-0.756	0.994	0.104	-0.982	-0.361	-0.147	0.999	0.995	0.998	0.999	0.876	0.998	0.99	0.995	0.994	0.998	1						
Yb	0.415	0.991	-0.759	0.686	-0.944	-0.858	-0.784	0.997	0.0608	-0.974	-0.401	-0.189	1	0.99	1	1	0.896	1	0.995	0.999	0.998	1	0.999	1					
Lu	0.387	0.995	-0.779	0.664	-0.953	-0.873	-0.765	0.995	0.0908	-0.98	-0.373	-0.159	0.999	0.993	0.999	0.999	0.883	0.999	0.992	0.997	0.995	0.999	1	1	1				
Hf	-1	-0.304	-0.263	-0.951	0.106	-0.097	0.897	-0.491	0.876	0.21	1	0.968	-0.434	-0.293	-0.45	-0.428	-0.784	-0.448	-0.515	-0.476	-0.49	-0.441	-0.389	-0.428	-0.401	1			
Pb	-0.0226	0.95	-0.967	0.301	-0.994	-0.996	-0.435	0.867	0.489	-0.976	0.0378	0.257	0.897	0.954	0.89	0.89	0.614	0.89	0.853	0.876	0.868	0.894	0.918	0.9	0.913	0.00792	1		
Th	-0.0672	0.935	-0.977	0.258	-0.987	-0.999	-0.395	0.844	0.528	-0.965	0.0823	0.3	0.877	0.939	0.868	0.88	0.578	0.869	0.829	0.853	0.845	0.873	0.9	0.88	0.894	0.0525	0.999	1	
U	0.582	0.947	-0.62	0.813	-0.863	-0.743	-0.888	0.993	-0.132	-0.912	-0.569	-0.374	0.983	0.943	0.986	0.981	0.965	0.985	0.996	0.99	0.992	0.984	0.972	0.981	0.975	-0.593	0.8	0.773	1

IV.   Origins and Enrichment of REEs

The mineral components of nodules viz. Fe and Mn minerals: todorokite: [(Na,Ca,K,Ba,Sr)1–*x*(Mn, Mg, Al)$_6$O$_{12}$·3-H$_2$O], goethite: FeOOH and few clay minerals, have large specific surface areas and strong adsorption of colloids. They promote the accumulation of REEs in the surrounding medium (Kanazawa and Kamitani 2006;Ran and Liu 1992;Liu et al. 2001;Wan and Liu. 2004). In addition, organic matter in polymetallic nodules additionally has a positive effect on REE enrichment (Meng and Fu. 2006;Li et al. 2005).

The Fe and Co are concentrated close to nucleus (hydrogenetic in origin), and Mn more concentrated in outer layers (early diagenetic) of nodules from CIOB (Jauhari and Pattan 2000). The enormously low Ce contents and low Ce anomalies (Zero to negative Ce anomaly) suggest that CIOB nodules might have formed in less oxidized environments than those of Pacific (González et al. 2010) and they had been formed at lower redox level in the vicinity of the redox boundary, and in settlement with a diagenetic growth and later exhumation process.

The nodules become rich in REEs which may exceed several times than that of regular marine sediments through the adsorption of REEs from seawater and sediment during the growth process of nodules. Piper 1974 studied that REEs in sediments are enriched in sediments through two main sources sediments viz. weathered terrigenous material and submarine volcanoes. Some other factors such as physical, chemical, biological and structural setup also affect the enrichment process of Fe-Mn nodules (Greta ME 1987; Richard and Margaret. 1993; Bruno et al. 1999; Karem et al. 2011).

The 90ºE Ridge along its enlargement supported the generation of submarine basalt and active hydrothermal fluids. The weathering of submarine basalt and hydrothermal fluids provide plenty of source material for the minerals in nodules and increasing the size of nodules. The concentration of Fe, Mn, Cu, Co, Ni, other metals and REEs is increased in water and sediment through the seabed volcanic eruptions (Sholkovitz et al. 1999; Zhang et al. 2008; Klinkhammer et al. 1994; Mascarenhas et al. 2010) and hydrolysis of submarine rock, prompting the growth and mineralization of nodules. The REE content in crusts is higher than that of nodules as evinced by the higher REE content in nodules at sea margins, which is in accordance with the adequate supply of terrestrial sediments. Infact, REE enrichment in marine nodules is a complex process, affected by the type of substance forming, sediments type, oceanic environments, and mineral characteristics (Cui et al. 2009; Ren et al., 2010; Jiang et al. 2011).

REEs very well adsorbed by the manganese oxides and hydroxides, helping their enrichment. The Ce shows different geochemistry as compared to other trivalent REEs, and it is easier to precipitate than other REEs. It exists in two valence states: Ce^{3+} and Ce^{4+}. In strongly oxidizing environments, the Ce^{4+} with a higher valency can be easily and strongly adsorbed by a solid material in seawater, and therefore more easily adsorbed by the nodules. It is due to this characteristic, Ce is not only strongly present in nodules, but is additionally often used to indicate the level of oxidation in the seawater environment indicating occurrence of nodules in oxidizing environments. The Ce enrichment in nodules causes the loss of calcium carbonate, barite, apatite, silica, and other sediments.

The abundance of chemical elements has been utilized in defining sediment sources, elucidating mechanisms of formation of the sediments, estimating the abundance of various components, quantifying authigenic deposition rates and fluxes of various elements, and in understanding depositional environments (Goldberg and Arrhenius 1958; S Krishnaswami 1976; Graybeal and Health. 1984; Thomson et al. 1984; Toyoda and Nakamura. 1990). In particular, the REE form a coherent group with trivalent oxidation state, besides for Ce, which oxidises to the tetravalent state and Eu, which reduces to the divalent state. REE are widely used as signs of various geochemical approaches which include depositional environment (Piper 1974; Taylor and McLennan 1985; Murray et al. 1992), redox conditions (Glasby et al. 1987; Liu et al. 1988), surface productivity (Toyoda et al. 1990), and to trace aeolian and hydrothermal input (Elderfield et al., 1988).

V.   Discussion

The average chemical composition of a nodule is inversely associated with its size. In comparison to their larger nodules the smaller nodules have a higher grade. Thus, we may also infer that except morphological characters, the small and large nodules are distinct in their compositions. The two different types of nodules, therefore, suggest two different modes of formation viz. by diagenetic and hydrogenetic processes (Valsangkar et al., 1992).

In the marginal sea, terrigenous sources contribute detritus to marine Fe-Mn deposits, whose characteristics are different from those of the other open oceans such as CIOB. The marginal sea Fe-Mn deposits are characterized by high precipitate growth rates, and they generally have relatively low Co, Ni, Cu, and Zn contents and Mn/Fe ratios (Conrad et al. 2017). The concentrations of Mn, Mo and Co however, show relatively high in comparison to continental crust.

The CIOB indicates slow rates of sediment accumulation because it is roughly 1600 km far from the southern tip of Indian peninsula and as a result, the CIOB is taken into consideration beneficial for Fe-Mn nodules mineralization. The hydrogenetic Fe-Mn deposits are enriched in Co, REEs (rare earth elements), Y, Te and Pt whereas the hydrothermal deposits are enriched in Mo, Zn and Ba, and the diagenetic deposits are

enriched in Mn, Cu, Mo and Ni (Hein et al. 2003;Hein et al. 2013b;Hein and Koschinsky 2014b;Bau et al. 2014a).

Table 8: Compositional Variations among Nodules of Different Size Classes (Values in %)											
	Size Class (<=4 cm)				Size Class (> 4 cm)				Sample of All Size Classes		
	Min	Max	Avg	SD	Min	Max	Avg	SD	Min	Max	Avg	SD
Mn	24.42	28.92	26.50	1.43	22.94	25.72	24.34	0.98	22.94	28.92	25.63	1.66
Fe	7.92	10.11	8.64	0.78	9.09	10.15	9.72	0.38	7.92	10.11	9.07	0.86
SiO$_2$	13.41	16.51	14.63	0.94	13.73	15.98	15.09	0.67	13.41	16.51	14.81	0.89
Al$_2$O$_3$	2.92	3.55	3.16	0.19	2.98	3.68	3.33	0.27	2.92	3.55	3.22	0.74
CaO	2.11	2.62	2.37	0.17	2.23	2.82	2.53	0.17	2.11	2.62	2.43	0.19
MgO	1.68	1.99	1.83	0.11	1.44	2.04	1.75	0.02	1.44	1.99	1.80	0.16
Na$_2$O	1.22	1.75	1.44	0.17	1.41	1.78	1.67	0.10	1.22	1.75	1.53	0.18
K$_2$O	0.89	1.19	1.03	0.10	1.04	1.21	1.11	0.05	0.89	1.19	1.06	0.09
Cu	1.02	1.22	1.13	0.07	1.01	1.11	1.05	0.03	1.02	1.22	1.10	0.07
Ni	0.98	1.24	1.09	0.09	0.97	1.08	1.00	0.03	0.97	1.24	1.05	0.08

Values in ppm											
TiO$_2$	6800	8300	7694	390	7400	8400	7917	276	6800	8400	7783	372
P$_2$O$_5$	2200	3800	2906	486	2700	3600	2625	375	2200	3800	3003	468
Zn	1400	1900	1633	160	1400	1700	1525	92	1400	1900	1500	149
Co	1600	2800	2090	350	2100	2800	2400	250	1600	2800	2230	296
Pb	900	1800	1244	313	1100	1800	1244	313	900	1800	1357	310
Sr	600	1400	906	321	900	1600	1350	189	600	1600	1103	308

The geochemical analysis and variations in Mn/Fe and Cu + Ni ratios among smaller nodules (<4 cm) to larger nodules (>4 cm) is 3.06 to 2.50 and 2.22 to 2.05 respectively (Table 8) suggest some variation in source and early diagenesis (Halbach et al. 1981;Valsangkar et al. 1988) and suggest more or less the uniformity of regional geochemical conditions. This ratio of Mn/Fe suggest that the nodules are of mixed origin i.e. authigenitic as well as diagenetic. This is further evident from the variation in Mn/Fe ratios in the study area where nodules have grown to different sizes with varying compositions. Therefore, variation in Mn/Fe ratio additionally helps the view that different sized nodules have formed differently at different places in various sedimentary environments. Formation of nodules by different accretionary processes is obvious from Fig. 6 and 7 wherein the plots spread from diagenetic to hydrogenetic field. It is, therefore, clear that these processes have beenresponsible for the formation of nodules, leading to distinguishable morphological, mineralogical and chemical properties. Owing to the fact that the different sized nodules occur near each other at the seafloor, it is not reasonable to consider that the above processes have been active either all at a time, alternatively or simultaneously in the area. This helps the view that the formation of different sized nodules took place separately in different areas (Valsangkar et al. 1988;Valsangkar et al. 1992). Thus, larger nodules which are poor in grade and Mn and Zn content suggest their formation specially from seawater and so, are rich in Fe and Co contents. Formation of smaller nodules by diagenetic process with an additional supply source (consistingof CCD) explains why they are higher in grade and Mn and Zn contents. It is possible that initially the nucleus of the nodule was formed at a shallower depth after which it changed into transported to deeper depth because of the currents along the downslope, where it grew slowly from the seawater (hydrogenous).

VI.   Conclusions

Large nodules form over a large nucleus and v*ice versa*. This in addition indicates that smaller nodules did not grow to the larger sizes, which shows that the processes of formation of smaller and larger nodules operate separately and that the larger nodules did not grow from smaller ones.

- Nodules of different size from CIOB have distinct geochemical, mineralogical and morphological Characteristics by which they can be distinguished as poor or high grades.
- Nodules of poor grade are large in size, formed in deeper water and hydrogenous in nature.
- Nodules of smaller size form at shallow depth and then may move towards deep areas.
- Average N/n ratio (size of nodule/size of nucleus) and nucleus size increase with increase in nodule size suggesting that smaller and bigger nodules form at different places by different accretionary processes.

Further, study indicates that there is high average abundance of Mn (25.63%), moderate Fe (8.91%) and low contents of trace metals and REEs compared to the average content of deep oceanic nodules from different other oceanic areas. Investigation for deep-sea nodule is involved in resource exploration, and advance scientific research. For either resources exploration or scientific research, precise geochemical analysis is very significant for the study. The present work determined V, Cr, Mn, Co, Ni, Zn, Rb, Sr, Nb, Mo, Cs, Ba, La, Ce, Pr, Nd, Sm, Eu, Gd, Dy, Ho, Er, Tm, Yb, Lu, Hf, Pb, Th and U in deep-sea nodules which proved that membrane desolation ICP-MS is a powerful multielement determination method in both exploration and research of deep-sea Fe-Mn nodules. This method, based on correct principle, with clear interference, authentic operation procedure with reliable results, can determine the concentrations of elements with potential economic value (Cr, Mn, Co, Ni and Zn) and the elements with important environmental significance (REE, U, Th, Rb, Sr and V), and will become an effective geochemical method for measuring micro and trace elements in Mn nodules. The nodules thus represent a strategic REE resource and will certainly catalyse further investigation of nodule resources in the CIOB. Comparatively, the REE in CIOB is less as the two main sources of REEs in sediments viz. weathered terrigenous material and submarine volcanoes are less in the study area.

References

[1]. AH Parulekar, SN Harkantra, ZA Ansari SM (1982) Abyssal benthos of the central Indian Ocean. Deep Sea Res part A 29:1531–1537

[2]. Alibo D, Acta YN (1999) Rare earth elements in seawater: particle association, shale-normalization, and Ce oxidation. geochemica Cosmochim actamicaca 63:363–372

[3]. Azmy K, Brand U, Sylvester P, et al (2011) Biogenic and abiogenic low-Mg calcite (bLMC and aLMC): Evaluation of seawater-REE composition, water masses and carbonate diagenesis. Chem Geol 280:180–190. https://doi.org/10.1016/j.ch

[4]. Baar H De, Brewer P, Acta MB-G et C, 1985 U (1985) Anomalies in rare earth distributions in seawater: Gd and Tb. geochemica Cosmochim acta 49:1961–1969

[5]. Baturin G (1988) The geochemistry of manganese andmanganese nodules in the ocean. Dordrecht, D. Reidel Publ Co

[6]. Bau M, Schmidt K, Koschinsky A, Hein, J; Kuhn, T; Usui A (2014a) Discriminating between different genetic types of marine ferro-manganese crusts and nodules based on rare earth elements and yttrium. Elsevier 381:1–9

[7]. Bau M, Schmidt K, Koschinsky A, Hein, J TK (2014b) Discriminating between different genetic types of marine ferro-manganese crusts and nodules based on rare earth elements and yttrium. Chem Geol 381:1–9

[8]. Bezrukov PL, Andrushchenko PF (1974) Geochemistry of Iron-Manganese Nodules from the Indian Ocean. Int Geol Rev 16:1044–1061. https://doi.org/10.1080/00206817409471781

[9]. Burns R, Burns V (1977) Mineralogy. In, Marine Manganese Deposits, ed. by GP GLASBY. Elsevier

[10]. Burns V, Letters RB-E and PS, 1978 U (1978a) Post-depositional metal enrichment processes inside manganese nodules from the north equatorial Pacific. Elsevier 39:341–348

[11]. Burns V, Mineralogist RB-A, 1978 U (1978b) Authigenic todorokite and phillipsite inside deep-sea manganese nodules. pubs.geoscienceworld.org 63:

[12]. Conrad T, Hein J, Paytan A, Clague D (2017) Formation of Fe-Mn crusts within a continental margin environment. Ore Geol Rev 87:25–40

[13]. Cronan, DS, Moorby S (1981) Manganese nodules and other ferromanganese oxide deposits from the Indian Ocean. J Geol Soc 138:527–539

[14]. Cronan D (1977) Deep-sea nodules: distribution and geochemistry. Oceanogr Ser 11–44

[15]. Cronan D, Hodkinson R, Geology SM (1991) Manganese nodules in the EEZ's of island countries in the southwestern equatorial Pacific. Mar Geol

[16]. Cronan DA (2006) Processes in the formation of Central Pacific manganese nodule deposits. J Mar Sci

[17]. Cui Y C, Liu J H, Ren X W SXF (2009) Geochemistry of rare earth elements in cobalt-rich crusts from the Mid-Pacific M seamount. Artic J Rare Earths 27:169–176. https://doi.org/10.1016/S1002-0721(08)60214-8

[18]. Dubinin A V, Shirshov PP (2004) Geochemistry of Rare Earth Elements in the Ocean. Lithol Miner Resour 39:289–307. https://doi.org/10.1023/B:LIMI.0000033816.14825.a2

[19]. Elderfield H, Whitfield M, Burton J D, Bacon M P LPS (1988) The oceanic chemistry of the rare-earth elements. Philos Trans R Soc London Ser A, Math Phys Sci 325:105–126. https://doi.org/10.1098/rsta.1988.0046

[20]. Frazer, JZ, Wilson L (1980) Manganese nodule resources in the Indian Ocean. Mar Min 2:257–292

[21]. Glasby, G. P, Keays, R. R, Rankin PC (1978) The distribution of rare earth, precious metal and other trace elements in Recent and fossil deep-sea manganese nodules

[22]. Glasby G, Gwozdz R, Kunzendorf, H GF (1987) The distribution of rare earth and minor elements in manganese nodules and sediments from the equatorial and SW Pacific. Lithos 20:97–113

[23]. Goldberg E, Arrhenius G (1958) Chemistry of Pacific pelagic sediments, Geochim. Cosmochim. Ac., 13, 153–212. Geochemica Cosmochim Acta 13:153–212

[24]. González FJ, Somoza L, Lunar R, et al (2010) Internal features, mineralogy and geochemistry of ferromanganese nodules from the Gulf of Cadiz: The role of the Mediterranean Outflow Water undercurrent. J Mar Syst 80:203–218. https://doi.org/10.1016/j.jmarsys.2009.10.010

[25]. GP Glasby (1977) Why manganese nodules remain at the sediment-water interface. New Zeal J Sci 20:187–190

[26]. Graybeal, AL GH (1984) Remobilization of transition metals in surficial pelagic sediments from the eastern Pacific. Geochemica

Cosmochim Acta 48:965–975

[27].   Guan Y, Sun X, Jiang X, et al (2017) The effect of Fe-Mn minerals and seawater interface and enrichment mechanism of ore-forming elements of polymetallic crusts and nodules from the South China Sea. Acta Oceanol Sin 36:34–46. https://doi.org/10.1007/s13131-017-1004-4

[28].   H.N Siddiquie, A.R Gujar, N.H Hashimi ABV (1984) Superficial mineral resources of the Indian Ocean. Deep Sea Res part A 31:763–812

[29].   Halbach P, Giovanoli, R DVB (1982) Geochemical processes controlling the relationship between Co, Mn, and Fe in early diagenetic deep-sea nodules. Earth Planet Sci Lett 60:226–236

[30].   Halbach P, Scherhag C, Hebisch U (1981) Geochemical and mineralogical control of different genetic types of deep-sea nodules from the Pacific Ocean. Miner Depos

[31].   Hein, J.R., Koschinsky, A., Bau, M., Manheim, F.T., Kang, J.K., Roberts, K. 2000 (2000) Cobalt-rich ferromanganese crusts in the Pacific. Handb Mar Miner Depos books.google.com

[32].   Hein J, Conrad T, Mizell, K VB (2016) Controls on ferromanganese crust composition and reconnaissance resource potential, Ninetyeast Ridge, Indian Ocean. Deep Sea Res Elsevier 110:1–19

[33].   Hein J, Koschinsky A (2014a) Deep-ocean ferromanganese crusts and nodules. Elsevier 13:273–291

[34].   Hein J, Koschinsky A (2014b) Deep-ocean ferromanganese crusts and nodules. Treatise Geochemistry Second Ed 13:273–291

[35].   Hein J, Spinardi F, Okamoto N, … KM (2015) Critical metals in manganese nodules from the Cook Islands EEZ, abundances and distributions. Ore Geol Rev

[36].   Hein JR, Koschinsky A, Halliday AN (2003) Global occurrence of tellurium-rich ferromanganese crusts and a model for the enrichment of tellurium. geochemica Cosmochim acta 67:1117–1127. https://doi.org/10.1016/S0016-7037(00)01279-6

[37].   Hein JR, Mizell K, Koschinsky A, et al (2013a) Deep-ocean mineral deposits as a source of critical metals for high-and green-technology applications: Comparison with land-based resources ARTICLE in ORE GEOLOGY REVIEWS · DECEMBER 2012 Deep-ocean mineral deposits as a source of critical metals for high-. Ore Geol Rev 51:1–14. https://doi.org/10.1016/j.oregeorev.2012.12.001

[38].   Hein JR, Mizell K, Koschinsky A, et al (2013b) Deep-ocean mineral deposits as a source of critical metals for high-and green-technology applications: Comparison with land-based resources ARTICLE in ORE GEOLOGY REVIEWS · DECEMBER 2012 Deep-ocean mineral deposits as a source of critical metals for high-. Ore Geol Rev 51:1–14. https://doi.org/10.1016/j.oregeorev.2012.12.001

[39].   Hlawatsch, S., Garbe-Schönberg, C.D., Lechtenberg, F., Manceau, A., Tamura, N., Kulik, D.A., Kersen M (2002) Trace metal fluxes to ferromanganese nodules from the western Baltic Sea as a record for long-term environmental changes. Chem Geol 182:697–709

[40].   Horn D, Ewing M, Horn, BM MD (1972) World-wide distribution of manganese nodules. Ocean Ind 7:26–29

[41].   Jarvis K, Gray A, Houk R (1997) Handbook of inductively coupled plasma mass spectrometry. agris.fao.org

[42].   Jauhari, P JP (2000) Ferromanganese nodules from the central Indian Ocean basin. Handb Mar Miner Depos 171–195

[43].   Jiang X, Wen L, Lin XDY (2011) Enrichment mechanism of rare earth element in marine diagenetic ferromanganese nodule. Mar Sci

[44].   Kanazawa Y, Kamitani M (2006) Rare earth minerals and resources in the world. J Alloys Compd 408:1339–1343. https://doi.org/10.1016/j.jallcom.2005.04.033

[45].   Klinkhammer G, Elderfield, H; Edmond, JM; Mitra A (1994) Geochemical implications of rare earth element patterns in hydrothermal fluids from mid-ocean ridges. geochemica Cosmochim acta 58:5105–5113

[46].   Koschinsky A, Bau M, Marbler H, et al (2010) Rare valuable metals in marine ferromanganese nodules-contents and accumulation process. Zeitschrift Angew Geol

[47].   Li J, Gong Z, Li Y, et al (2005) Geochemical behaviors of rare earth elements in the estuary of Changjiang River in China. Acta Oceanol Sin 27:164

[48].   Liu C, Wu J, Yu W (2001) Controls of interactions between iron hydroxide colloid and water on REE fractionations in surface waters: Experimental study on pH-controlling mechanism. Sci China, Ser D Earth Sci 45:449–458. https://doi.org/10.1360/02yd9047

[49].   Liu Y, Miah, MRU RS (1988) Cerium: a chemical tracer for paleo-oceanic redox conditions. Geochemica Cosmochim Acta 52:1361–1371

[50].   MBL Mascarenhas-Pereira BN (2010) Selective leaching studies of sediments from a seamount flank in the Central Indian Basin: Resolving hydrothermal, volcanogenic and terrigenous sources. Mar Chem 121:49–66

[51].   Meng, Y MF (2006) Capacity change of marine sediments with and without organic matter for absorption of rare earth elements. J Trop Oceanogr 25:20

[52].   Mukhopadhyay R (1987) Morphological variations in the polymetallic nodules from selected stations in the Central Indian Ocean. Geo-Marine Lett 7:45–51

[53].   Murray R, Brink, MRB ten DG (1992) Interoceanic variation in the rare earth, major, and trace element depositional chemistry of chert: perspectives gained from the DSDP and ODP record. Geochemica Cosmochim Acta 56:1892–1913

[54].   Nath B, Balaram V, Sudhakar, M WP (1992) Rare earth element geochemistry of ferromanganese deposits from the Indian Ocean. Mar Chem 38:185–208

[55].   Pattan, JN, Kodagali V (1988) Seabed topography and distribution of manganese nodules in the Central Indian Ocean. Mahasagar 21:

[56].   Pattan, JN VB (1993) Rare earth element distribution and behaviour in buried manganese nodules from the Central Indian Basin. Mar Geol 112:303–312

[57].   Piper DZ (1974) RARE EARTH ELEMENTS IN THE SEDIMENTARY CYCLE: A SUMMARY

[58].   Ran Y LZ (1992) Contents and distribution of rare earth elements in main types of soils in China. J Rare Earths 12:248

[59].   Rao V (1987) Mineralogy of polymetallic nodules and associated sediments from the Central Indian Ocean Basin. Mar Geol 74:151–157

[60].   Ren X W, Shi X F, Zhu A M, Liu J H FXS (2010) Controlling Factors on Enrichment of Cerium in Co-Rich Fe-Mn Crusts from Magellan Seamount Cluster. J Chinese Rare Earths Soc 28:489

[61].   Reynard B, Lécuyer C, Grandjean P (1999) Crystal-chemical controls on rare-earth element concentrations in fossil biogenic apatites and implications for paleoenvironmental reconstructions. Chem Geol 155:233–241. https://doi.org/10.1016/S0009-2541(98)00169-7

[62].   Reyss J, Lemaitre N, Ku, TL VM (1985) Growth of a manganese nodule from Peru Basin: A radiochemical anatomy. Geochemica Cosmochim Acta 49:2401–2408

[63]. Richard W M ML (1993) Chemical transport to the seafloor of the equatorial Pacific Ocean across a latitudinal transect at 135 W: tracking sedimentary major, trace, and rare earth element. Geochemica Cosmochim Acta 57:4141–4163

[64]. S Krishnaswami (1976) Authigenic transition elements in Pacific pelagic clays. Geochemica Cosmochim Acta 40:425–435

[65]. Shan, L and D Y (1993) Mineral facies changes and secondary changes in ferro-manganese nodules. acta Mineral Sin 13:150–162

[66]. Sholkovitz E (1988) Rare earth elements in the sediments of the North Atlantic Ocean, Amazon Delta, and East China Sea; reinterpretation of terrigenous input patterns to the. Am J Sci 288:236–281

[67]. Sholkovitz E (1990) Rare-earth elements in marine sediments and geochemical standards. Chem Geol 88:333–347

[68]. Sholkovitz E, Elderfield H, Szymczak R, Chemistry KC (1999) Island weathering: river sources of rare earth elements to the Western Pacific Ocean. Mar Chem 68:39–57

[69]. Sholkovitz E, Landing W, Acta BL (1994) Ocean particle chemistry: the fractionation of rare earth elements between suspended particles and seawater. Geochemica Cosmochim Acta 58:1567–1579

[70]. Siddiquie H, Gupta D, Sengupta N (1978) Manganese-iron nodules from the Indian Ocean. Indian J Mar Sci 7:239–253

[71]. Takahashi Y, Manceau A, Geoffroy N, et al (2007) Chemical and structural control of the partitioning of Co, Ce, and Pb in marine ferromanganese oxides. Geochemica Cosmochim Acta 71:984–1008. https://doi.org/10.1016/j.gca.2006.11.016

[72]. Taylor S, McLennan S (1985) The continental crust: its composition and evolution. Blackwell London

[73]. Thomson J, Carpenter MSC (1984) Metal accumulation rates in northwest Atlantic pelagic sediments. Geochemica Cosmochim Acta 1935–1948

[74]. Toyoda K, Nakamura, Y AM (1990) Rare earth elements of Pacific pelagic sediments. Geochemica Cosmochim Acta 54:1093–1103

[75]. Usui, A & Someya M (1997) Distribution and composition of marine hydrogenetic and hydrothermal manganese deposits in the northwest Pacific. Geol Soc London 119:177–198

[76]. Valsangkar, AB, Khadge N (1989) Size analyses and geochemistry of ferromanganese nodules from the Central Indian Ocean Basin. Mar Min 8:325–347

[77]. Valsangkar A, Khadge, NH JDE (1992) Geochemistry of polymetallic nodules from the Central Indian Ocean Basin. Mar Geol 103:361–371

[78]. Valsangkar A, Rajamanickam, GV SK (1988) Morphological and interlayer geochemical studies on manganese nodules from the southwestern Carlsberg Ridge. Mar Geol Elsevier 84:81–94

[79]. Verlaan P, Cronan, DS CM (2004) A comparative analysis of compositional variations in and between marine ferromanganese nodules and crusts in the South Pacific and their environmental. Prog Oceanogr 63:125–158

[80]. Wan Y X LCQ (2004) Study on adsorption of rare earth elements by kaolinite. J Rare Earths 22:507

[81]. Wegorzewski, AV TK (2014) The influence of suboxic diagenesis on the formation of manganese nodules in the Clarion Clipperton nodule belt of the Pacific Ocean. Mar Geol 357:123–138

[82]. Wiltshire JC, Yuan Wen X, Yao D (1999) Marine Georesources and Geotechnology Ferromanganese Crusts near Johnston Island: Geochemistry, Stratigraphy and Economic Potential. Taylor Fr 17:257–270. https://doi.org/10.1080/106411999273936

[83]. Xia, N; S, Song; D, Yao; Z, Jiang; L J (2001) Determination of adsorbed water in polymetallic nodules. rock Miner Anal 20:263–266

[84]. Xu Z K, Li A C, Xu F J, Meng Q Y, Li C S LJG (2007) Elemental occurrence phases of surface sediments from the East Philippine Sea. CHINA Int B … 27:51

[85]. Yao, D; L, Zhang; J, Wiltshire; C, Morgan; R C (1996) Mineralogy and geochemistry of ferromanganese crusts from Johnston Island EEZ. ieeexplore.ieee.org 16:33–49

[86]. Yao, D., H. Liang, L. Zhang and DX (1993) Rare earth element geochemistry of polymetallic nodules from the central Pacific. Oceanol Limnol Sin 24:571–576

[87]. Zhang Y, Lacan, F CJ (2008) Dissolved rare earth elements tracing lithogenic inputs over the Kerguelen Plateau (Southern Ocean). Deep Sea Res Part II 55:638–652

[88]. Zhang Z, Yuansheng D, Lianfeng, GA YZ (2012a) Enrichment of REEs in polymetallic nodules and crusts and its potential for exploitation. J Rare Earths 30:621–626

[89]. Zhang Z, Yuansheng D, Lianfeng, GAO YZ (2012b) Enrichment of REEs in polymetallic nodules and crusts and its potential for exploitation. J Rare Earths 30:621–626